



**NAM**

# **Empirical Ground-Motion Prediction Equations for Peak Ground Velocity from Small-Magnitude Earthquakes in the Groningen Field Using Multiple Definitions of the Horizontal Component of Motion**

---

**Julian J Bommer, Peter J Stafford & Michail Ntinalexis**

Datum November 2016

Editors Jan van Elk & Dirk Doornhof



## General Introduction

The hazard from induced earthquakes is primarily presented by the ground motion to which buildings and people are subjected. The prediction of ground motion, resulting from the earthquakes in the Groningen area induced by the production of gas, is critical for the assessment and prognosis of building damage and personal risk.

The research into the development of the ground motion prediction methodology started in 2012 and continues as more ground motion data from Groningen earthquakes is being collected. The prime goal of these studies has been the assessment of ground motion for risk assessment. This means the focus has very much been on the prediction of ground acceleration for larger events, extrapolating from the currently available data obtained from earthquakes with magnitude below  $M=3.6$  to earthquakes with magnitude in the range from  $M=4$  to 5 and up to  $M_{\max}$  (Ref. 1). The development of these Ground Motion Prediction Models has been documented in several reports (Ref. 2, 3 and 4).

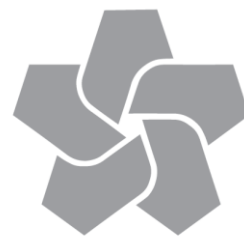
Additionally, a Ground Motion prediction methodology was developed for smaller earthquakes within the range of experience. This methodology was developed for operational use within the context of a new damage protocol. This methodology therefore aims to accurately predict ground motion for earthquakes in the same range as the historical data base, primarily from  $M=2.0$  to  $M=3.0$ . Additional to the peak ground acceleration this methodology also covers peak ground velocity and  $V_{top}$ . These last two metrics of ground motion are especially relevant for building damage and comparison with the Guidelines of the SBR (Stichting Bouw Research) (Ref. 5 and 6).

### References:

1. Report on Mmax Expert Workshop, Mmax panel chairman Kevin Coppersmith, June 2016
2. Technical Addendum to the Winningsplan Groningen 2013; Subsidence, Induced Earthquakes and Seismic Hazard Analysis in the Groningen Field, Nederlandse Aardolie Maatschappij BV (Jan van Elk and Dirk Doornhof, eds), November 2013.
3. Development of Version 1 GMPEs for Response Spectral Accelerations and for Strong-Motion Durations, Julian J Bommer, Peter J Stafford, Benjamin Edwards, Michail Ntinalexis, Bernard Dost and Dirk Kraaijpoel, March 2015.
4. Development of Version 2 GMPEs for Response Spectral Accelerations and Significant Durations for Induced Earthquakes in the Groningen field, Julian J Bommer, Bernard Dost, Benjamin Edwards, Adrian Rodriguez-Marek, Pauline P Kruiver, Piet Meijers, Michail Ntinalexis & Peter J Stafford, October 2015
5. Meet- en beoordelingsrichtlijn: Trillingen - Deel B Hinder voor personen, Stichting Bouw Research, 2006.
6. Meet- en beoordelingsrichtlijn: Trillingen - Deel A Schade aan gebouwen, Stichting Bouw Research, 2010.

These reports are also available at the study reports page of the website [www.namplatform.nl](http://www.namplatform.nl).





**NAM**

<b>Title</b>	<b>Empirical Ground-Motion Prediction Equations for Peak Ground Velocity from Small-Magnitude Earthquakes in the Groningen Field Using Multiple Definitions of the Horizontal Component of Motion</b>		<b>Date</b>	November 2016		
<b>Autor(s)</b>	Julian J Bommer, Peter J Stafford & Michail Ntinalexis	<b>Editors</b>	Jan van Elk & Dirk Doornhof			
<b>Organisation</b>	Researcher primarily from Imperial College, London.	<b>Organisation</b>	NAM			
<b>Place in the Study and Data Acquisition Plan</b>	<u>Study Theme:</u> Ground Motion Prediction <u>Comment:</u> The prediction of Ground Motion is central to the hazard assessment. This report describes a Ground Motion Prediction methodology for operational use in the damage protocol, covering the magnitude range from M=2 to M=3.					
<b>Directly linked research</b>	(1) Hazard Assessment. (2) Fragility assessment of buildings in the Groningen region.					
<b>Used data</b>	Accelerograms from the accelerometers placed in the Groningen field. Description of the shallow geology of Groningen.					
<b>Associated organisation</b>	Imperial College (London).					
<b>Assurance</b>	Internal to the Hazard Team.					



# **Empirical Ground-Motion Prediction Equations for Peak Ground Velocity from Small-Magnitude Earthquakes in the Groningen Field Using Multiple Definitions of the Horizontal Component of Motion**

Julian J Bommer, Peter J Stafford & Michail Ntinalexis

A report to NAM

**November 2016**

## Table of Contents

1. Introduction and Scope	1
2. Ground-Motion Database	2
2.1. Groningen recordings	2
2.2. Values of peak ground velocity	4
3. Empirical Equations for PGV	8
3.1. Functional form	9
3.2. Regression analysis and residuals	10
3.3. Predictions of PGV	12
4. Concluding Remarks	15
5. References	15

## 1. Introduction and Scope

As part of its response to induced earthquakes in the Groningen gas field, NAM has requested an equation for the prediction of peak ground velocity (PGV). The current (V3) ground-motion model that has been developed for the NAM seismic hazard and risk modelling effort predicts response spectral accelerations at a range of oscillator periods from 0.01 s (which may be assumed equivalent to peak ground acceleration, PGA) to 5 seconds (Bommer *et al.*, 2016). The next phase of development of the Groningen ground-motion model (GMM) will include the incorporation of extended rupture effects, particularly for larger earthquakes, and also a model for the prediction of PGV.

However, the target for delivery of the V4 GMM is Q1 2017 and NAM does have an immediate requirement for a model to predict PGV values due to the small-magnitude earthquakes occurring in the field. The reason for this is that PGV is the basis of official Dutch guidelines for assessing the impact of vibration on buildings, as presented in the document *Building Damage: Measurement and Assessment* (SBR, 2002). Consequently, NAM has requested Groningen-specific GMPEs for PGV to estimate the value of this parameter at specific locations due to induced events in the field.

An important feature of the model requested by NAM for immediate application is that the equation only needs to be applicable to smaller magnitude earthquakes (*i.e.*, in the range of the events that have been recorded to date, the largest of which had a local magnitude,  $M_L$ , of 3.6 and moment magnitude,  $M$ , of 3.4). This differs from the main GMM, which is intended to be applicable up to magnitudes beyond 6.5, for which reason it includes logic-tree branches to accommodate the inevitable epistemic uncertainty associated with such extrapolation.

Another important difference between the model required by NAM and the main GMM is the definition of the horizontal component of motion. There are several options for obtaining a single value of acceleration or velocity from the two orthogonal horizontal components of an accelerogram (*e.g.*, Beyer & Bommer, 2006). For the main GMM, the standard definition of the geometric mean component is adopted for the hazard calculations, with an adjustment to the arbitrary component for the risk calculations, the difference between the two definitions being that the standard deviation of the latter includes the component-to-component variability; the median values are identical (Baker & Cornell, 2006). For NAM's current purposes, however, and for the consistency with the  $V_{TOP}$  parameter used in the relevant guidelines, the 'maximum' value of PGV is required. Since there is some uncertainty as to exactly which 'maximum' corresponds to the  $V_{TOP}$  definition, equations have been derived for two alternative definitions of the largest component; for completeness an equation for the geometric mean component is also included.

This report briefly summarises the derivation of these new equations, which supersede and replace the earlier models presented in April 2016. Following this introduction, Section 2 provides an overview of the database of ground-motion recordings used to derive the equations. The derivation of the models is then presented in Section 3, and the report closes with a brief discussion in Section 4.

## 2. Ground-Motion Database

In this section, the database used to derive the new PGV equations is briefly described, both in terms of its general characteristics and the values of PGV.

### 2.1. Groningen recordings

The database of recordings used to derive the PGV prediction equations is essentially the same as that used in the derivation of the V3 GMM (Bommer *et al.*, 2016). These are 178 recordings from 22 earthquakes in the Groningen field, obtained by surface accelerographs operated by KNMI (Figure 2.1). The earthquakes have local magnitudes,  $M_L$ , determined by KNMI between 2.5 and 3.6 (Table 2.1). In the derivation of the earlier PGV model, only recordings from the B-stations were considered because of the measured  $V_s$  profiles at these locations. Since it was found that the influence of  $V_{S30}$  in the predictions is almost negligible (see Section 3.1), for the current model the expanded database from both networks has been used.

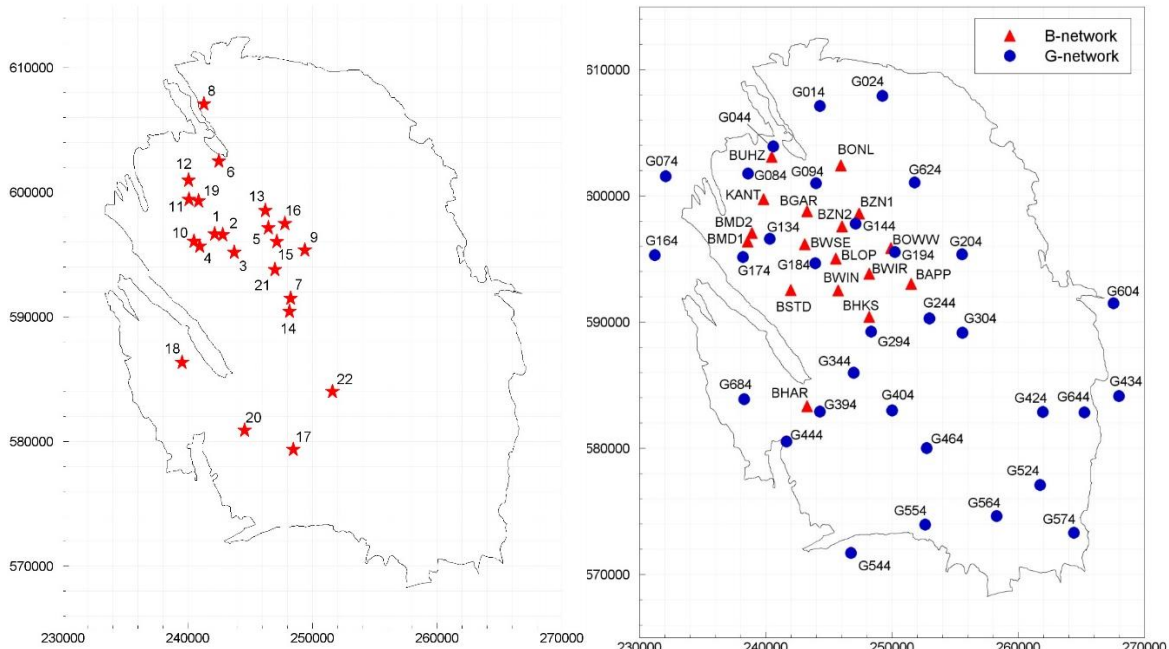


Figure 2.1. Location of the accelerograph stations in the Groningen field.

Table 2.1. Earthquakes producing records from the Groningen accelerograph network

EQ ID	Date			Time		M <sub>L</sub>	WGS84		RD Coordinates		Name
	Y	M	D	H	M		N°	E°	X (m)	Y (m)	
01	2006	VIII	8	05	04	3.5	53.350	6.697	242,159	596,659	Westeremden
02	2006	VIII	8	09	49	2.5	53.350	6.707	242,826	596,579	Westeremden
03	2008	X	30	05	54	3.2	53.337	6.720	243,740	595,168	Westeremden
04	2009	IV	14	21	05	2.6	53.342	6.678	240,955	595,673	Huizinge
05	2009	V	8	05	23	3.0	53.354	6.762	246,479	597,129	Zeerjip
06	2010	VIII	14	07	43	2.5	53.403	6.703	242,496	602,509	Uithuizermeeden
07	2011	VI	27	15	48	3.2	53.303	6.787	248,253	591,487	Garrelsweer
08	2011	VIII	31	06	23	2.5	53.444	6.687	241,305	607,070	Uithuizen
09	2011	IX	VI	21	48	2.5	53.338	6.805	249,399	595,368	Oosterwijterd
10	2012	VIII	16	20	30	3.6	53.345	6.672	240,504	596,073	Huizinge
11	2013	II	7	22	31	2.7	53.375	6.667	240,112	599,405	Zandeweer
12	2013	II	7	23	19	3.2	53.389	6.667	240,085	600,945	Zandeweer
13	2013	II	9	05	26	2.7	53.366	6.758	246,230	598,516	t Zandt'
14	2013	VII	02	23	03	3.0	53.294	6.785	248,163	590,446	Garrelsweer
15	2013	IX	04	01	33	2.8	53.344	6.772	247,166	596,048	Zeerjip
16	2014	II	13	02	13	3.0	53.357	6.782	247,804	597,489	Leermens
17	2014	IX	1	07	17	2.6	53.194	6.787	248,489	579,359	Froombosch
18	2014	IX	30	11	42	2.8	53.258	6.655	239,565	586,336	Garmerwolde
19	2014	XI	5	1	12	2.9	53.374	6.678	240,890	599,307	Zandeweer
20	2014	XII	30	2	37	2.8	53.208	6.728	244,561	580,898	Woudbloem
21	2015	I	6	6	55	2.7	53.324	6.678	246,987	593,800	Wirdum
22	2015	IX	30	18	05	3.1	53.258	6.800	251,603	584,016	Hellum

The magnitude-distribution of the recordings is shown in Figure 2.2, from which it can be appreciated that from M<sub>L</sub> 2.5 to 3.6 and for distances up to about 20-25 km, the distribution is reasonably good. Therefore, empirical models derived from these data are likely to perform well within these limits; the applicability of the models is discussed in Section 4.

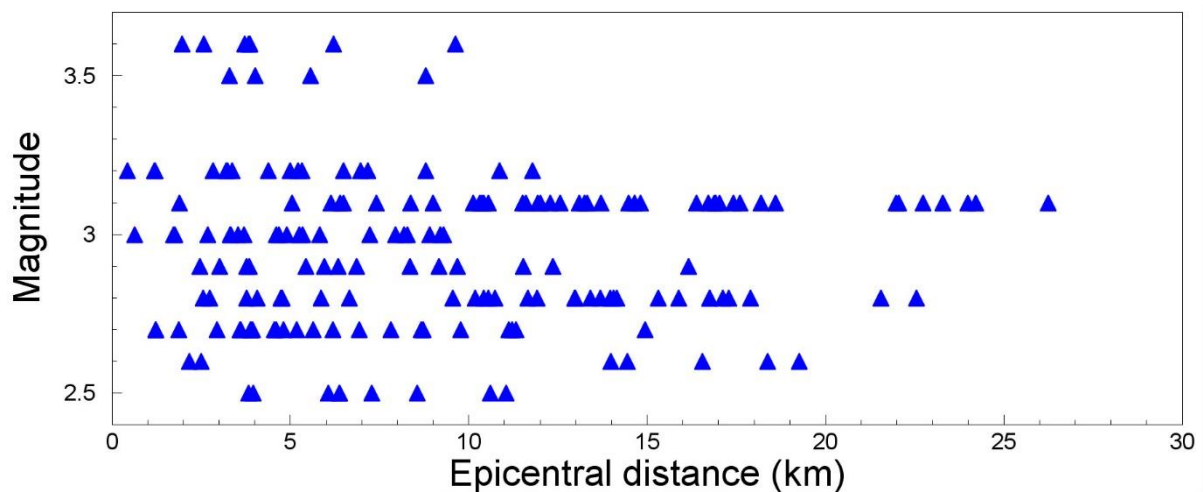


Figure 2.2. Magnitude-distance distribution of the data

## 2.2. Values of peak ground velocity

The largest recorded value of PGV on any single component within the database is 3.46 cm/s, which was on the NS component of the MID1 recording obtained at 2 km from the epicentre of the 2012 Huizinge M<sub>L</sub> 3.6 earthquake. Overall, the amplitudes of PGV are rather small, with only 14 of the 178 records have a PGV above 1 cm/s; for about half of the data, the recorded PGV values do not exceed 0.1 cm/s.

As noted in Section 1, three different definitions of the horizontal component of motion are considered in this study. If we label the PGV values on the two horizontal components of each recording as  $PGV_{NS}$  and  $PGV_{EW}$ , the geometric mean value of PGV is given by:

$$PGV_{GM} = \sqrt{PGV_{NS} PGV_{EW}} = \exp\left[\frac{\ln(PGV_{NS}) + \ln(PGV_{EW})}{2}\right] \quad (2.1)$$

The larger component, which in many early ground-motion studies was referred to as the maximum component, is simply the larger of the two as-recorded values of PGV:

$$PGV_{Larger} = \max[PGV_{NS}, PGV_{EW}] \quad (2.2)$$

Both of the two preceding definitions are constrained by the orientation of the recording instrument, which is unlikely to be aligned with the direction of the strongest shaking. In order to find the direction of maximum motion, the two components can be rotated through small angles (e.g., 1°) to find the rotated component with the largest peak on the velocity trace (e.g., Watson-Lamprey & Boore, 2007). For a single parameter, such as PGV, this can also be found from the following operation on the two orthogonal velocity traces:

$$PGV_{RotMax} = \max\left[\sqrt{V_{NS}(t)^2 + V_{EW}(t)^2}\right] \quad (2.3)$$

Applying this definition to all of the records results in a database of higher values, with the largest single PGV value—corresponding to the same MID1 recording of the Huizinge earthquake—now being 4.1 cm/s. The PGV values obtained applying both the larger component and the maximum rotated components are shown in Figure 2.3 plotted against distance.

Figures 2.4, 2.5 and 2.6 show the ratios of the PGV values obtained using the three different definitions. Immediately apparent are the very large differences between the geometric mean values and either of the two definitions that capture the ‘maximum’ component of motion. To a large extent these ratios are a result of the highly polarised nature of the Groningen motions, particularly when recorded at short distances, which

has been interpreted as most likely being a result of the radiation pattern from the earthquake source (Bommer *et al.*, 2016). The differences between the larger and maximum rotated components is smaller but still appreciable in many cases. As would be expected, the geometric mean definition yields the smallest values and the maximum rotated component the largest, even though there are ratios close to unity in several cases. The order of the three definitions is also confirmed by the plot in Figure 2.7.

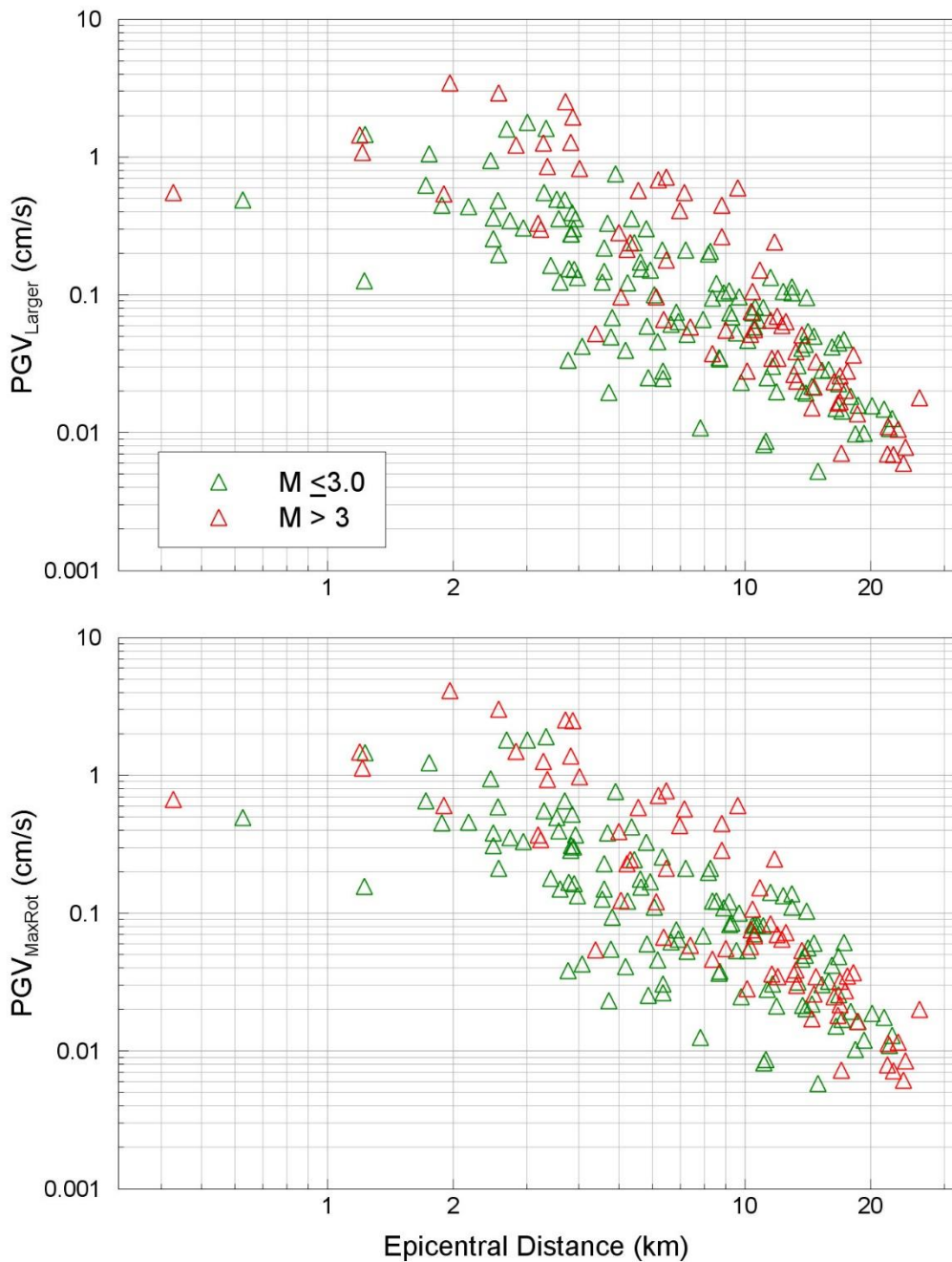


Figure 2.3. Values of larger and maximum rotated PGV against epicentral distance, and also grouped by the magnitude range of the earthquakes

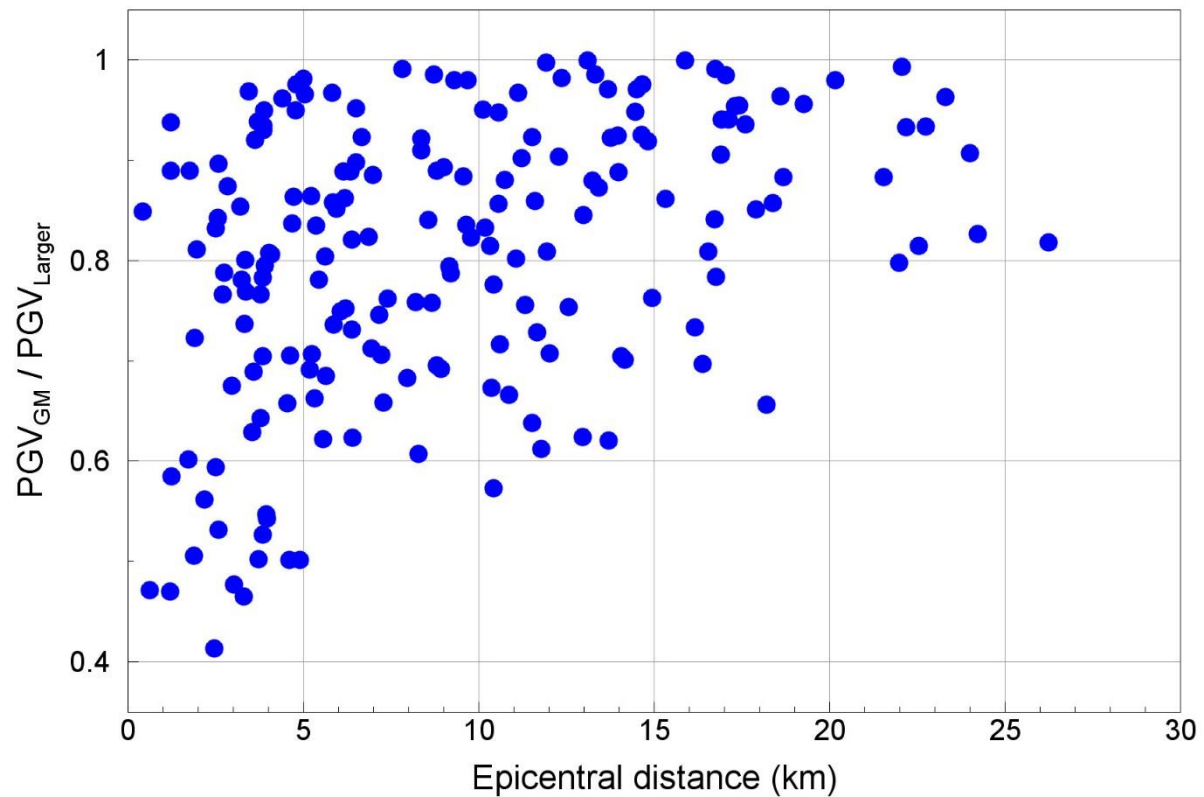


Figure 2.4. Ratios of geometric mean to larger PGV against epicentral distance

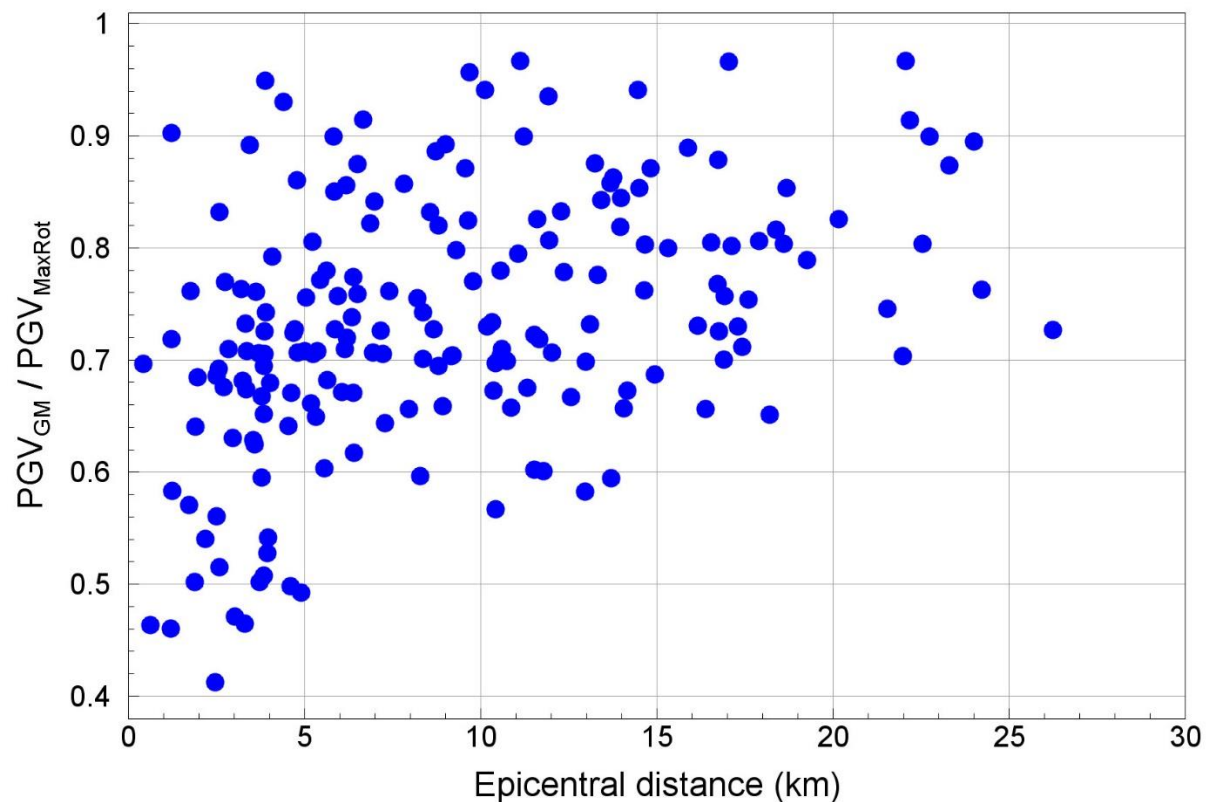


Figure 2.5. Ratios of geometric mean to maximum rotated PGV against epicentral distance

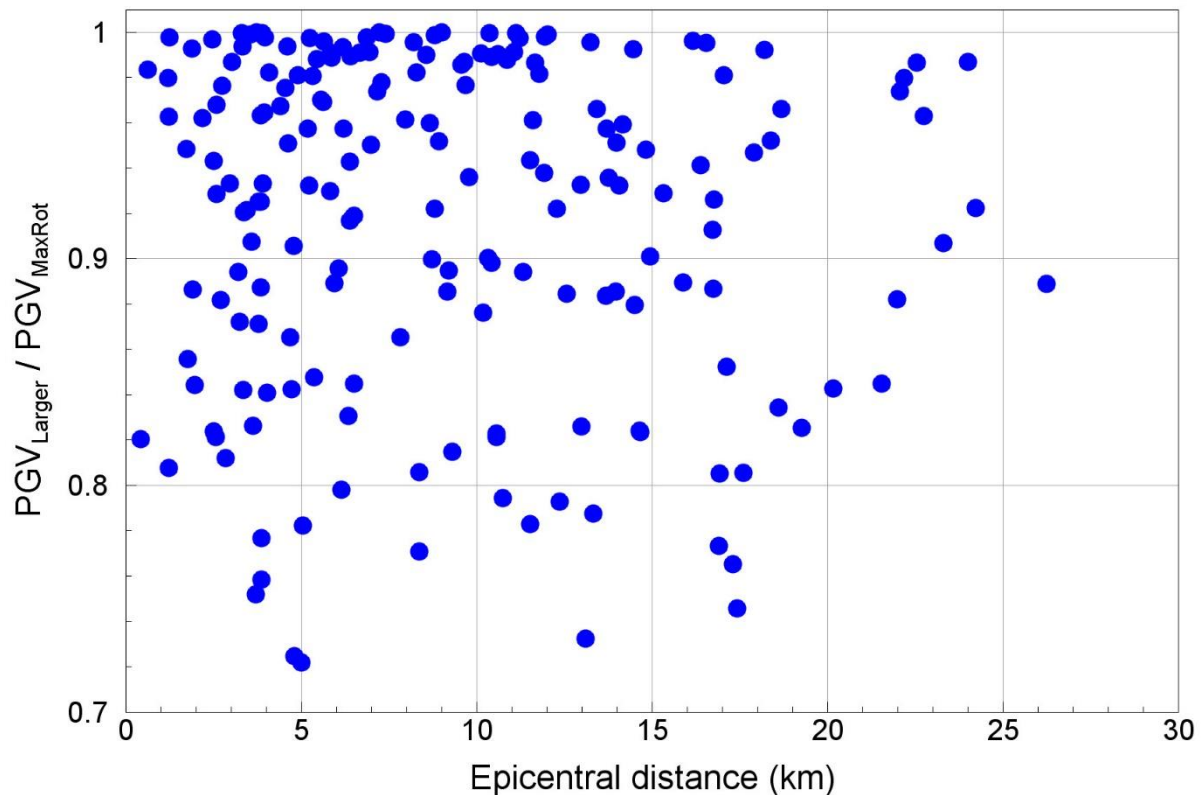


Figure 2.6. Ratios of larger to maximum rotated PGV against epicentral distance

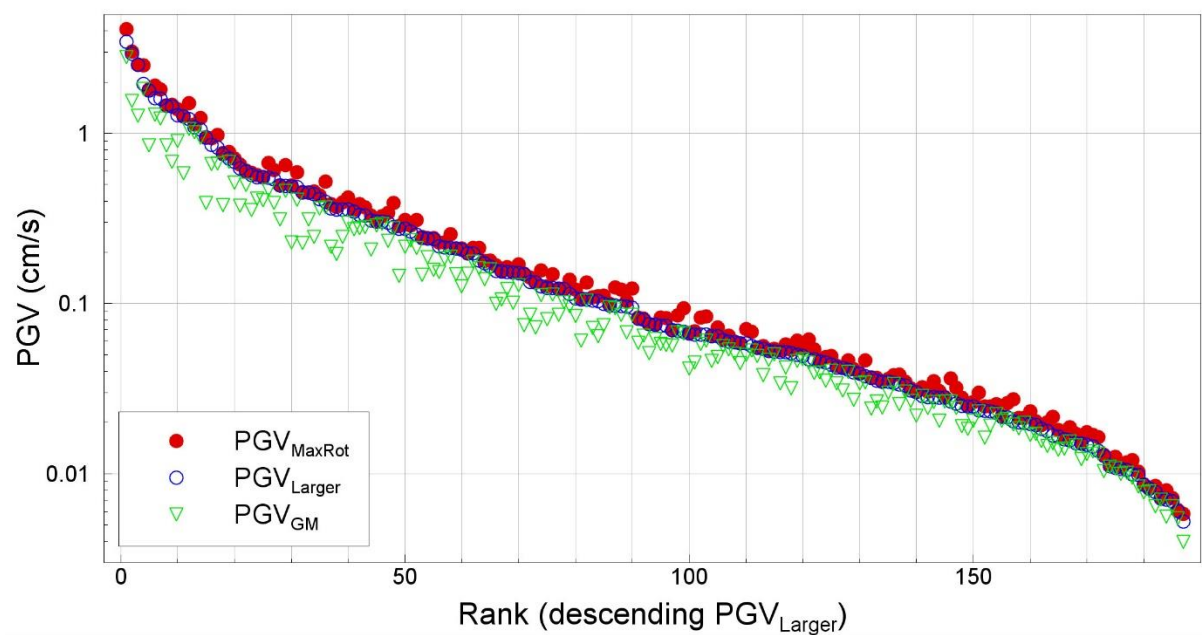


Figure 2.7. PGV values from all the 178 records determined using the three different definitions of the horizontal component of motion used in this study; note the logarithmic y-axis, which partially conceals the differences within each triplet of values

Another definition of horizontal PGV could be considered and this would be the Pythagorean of the two individual PGV values:

$$PGV_{Pyth} = \sqrt{PGV_{NS}^2 + PGV_{EW}^2} \quad (2.4)$$

This is effectively the same as the maximum rotated in the case that the peaks on the two components occur at exactly the same time. In all other cases, it is a conservative over-estimate the maximum motion. Figure 2.8 shows the ratios of maximum rotated PGVs to values calculated using this definition, from which it can be appreciated that they tend to differ more at greater distances and for weaker motions. These both correspond to situations in which the two horizontal peaks are less likely to be synchronous. For stronger motions, the ratios are closer to one, and for recorded PGV values greater than 1 cm/s, the ratios are consistently above 0.9. We do not believe that it would be justifiable to use the PGV values obtained by applying Eq.(2.4) hence equations are derived only for the three definitions already discussed.

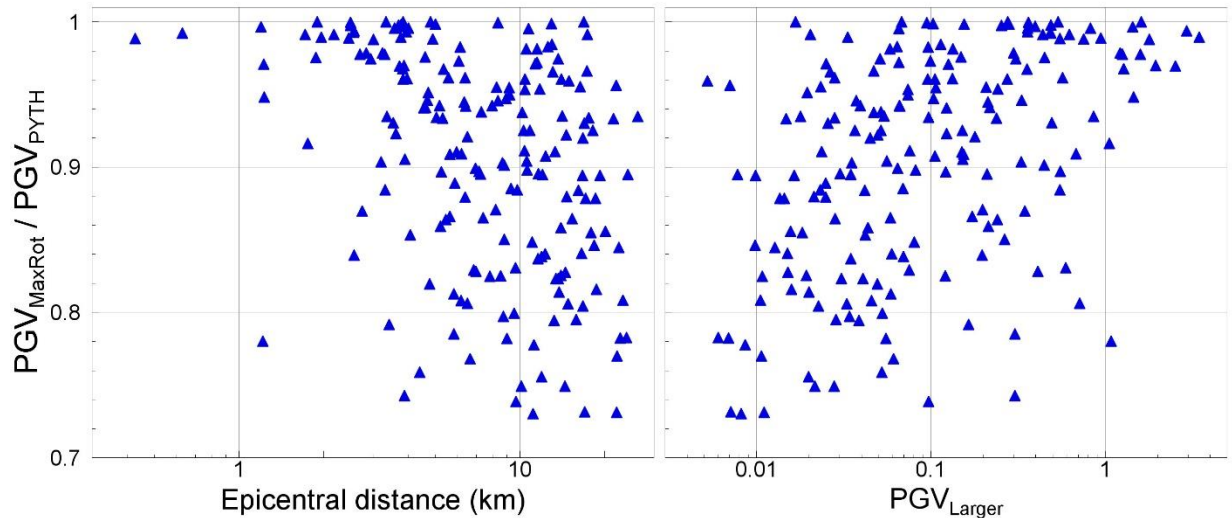


Figure 2.8. Ratios of the maximum rotated PGV to the PGV value obtained from the vector of the two individual horizontal peaks plotted against epicentral distance (*left*) and against the larger recorded value of PGV (*right*).

### 3. Empirical Equations for PGV

Using the database described in the previous section, empirical equations have been derived for the prediction of three definition of PGV. This section describes the derivation of these equations, starting with the selection of the functional form, followed by an explanation of the results of the regression analyses. The final sub-section illustrates the resulting equations in terms of predicted values of PGV.

### 3.1. Functional form

Although a simple V1-style equation was requested, it was considered appropriate to benefit from the advances in ground-motion modelling for the Groningen field that have been made as part of the seismic hazard and risk modelling project. Informed by the V2 GMM (Bommer *et al.*, 2015), as also used for the preliminary (April 2016) PGV equation, a suitable functional form was found to be as follows:

$$\ln(PGV) = c_1 + c_2 M + g(R) \quad (3.1)$$

with PGV in cm/s, M being local magnitude determined by KNMI and the distance term, R, is defined as in Eq.(3.2), namely:

$$R = \sqrt{R_{epi}^2 + [\exp(0.4233M - 0.6083)]^2} \quad (3.2)$$

The magnitude-dependent distance saturation term in Eq.(3.2) was obtained from regressions on Groningen recordings. The geometrical spreading term is segmented over three distances:

$$g(R) = c_4 \ln(R) \quad R \leq 6.32\text{km} \quad (3.3a)$$

$$g(R) = c_4 \ln(6.32) + c_{4a} \ln\left(\frac{R}{6.32}\right) \quad 6.32 < R \leq 11.62\text{km} \quad (3.3b)$$

$$g(R) = c_4 \ln(6.32) + c_{4a} \ln\left(\frac{11.62}{6.32}\right) + c_{4b} \ln\left(\frac{R}{11.62}\right) \quad R > 11.62\text{km} \quad (3.3c)$$

The distances separating the different segments of geometrical spreading were constrained by full waveform modelling using finite differences as undertaken by Ewoud van Dedem of Shell.

In the derivation of the preliminary PGV model in April 2016,  $V_{S30}$  (the 30-metre time-average shear-wave velocity at the site in m/s) was considered as an explanatory variable in addition to magnitude and distance. The results of the regression, however, showed that the influence of this parameter was almost negligible within the range of  $V_{S30}$  values encountered in the Groningen field (Figure 3.1). For this reason, and at NAM's specific request, the 30 m shear-wave velocity was not included as predictor variable in the new equations. This decision also simplifies the implementation of the equations in practice since it obviates the need to determine the  $V_{S30}$  value at each location of interest when estimating PGV values. All that is needed as inputs to the equations are the earthquake magnitude, as provided by KNMI, and the epicentral distance, which is very easily calculated, particularly in the RD coordinate system.

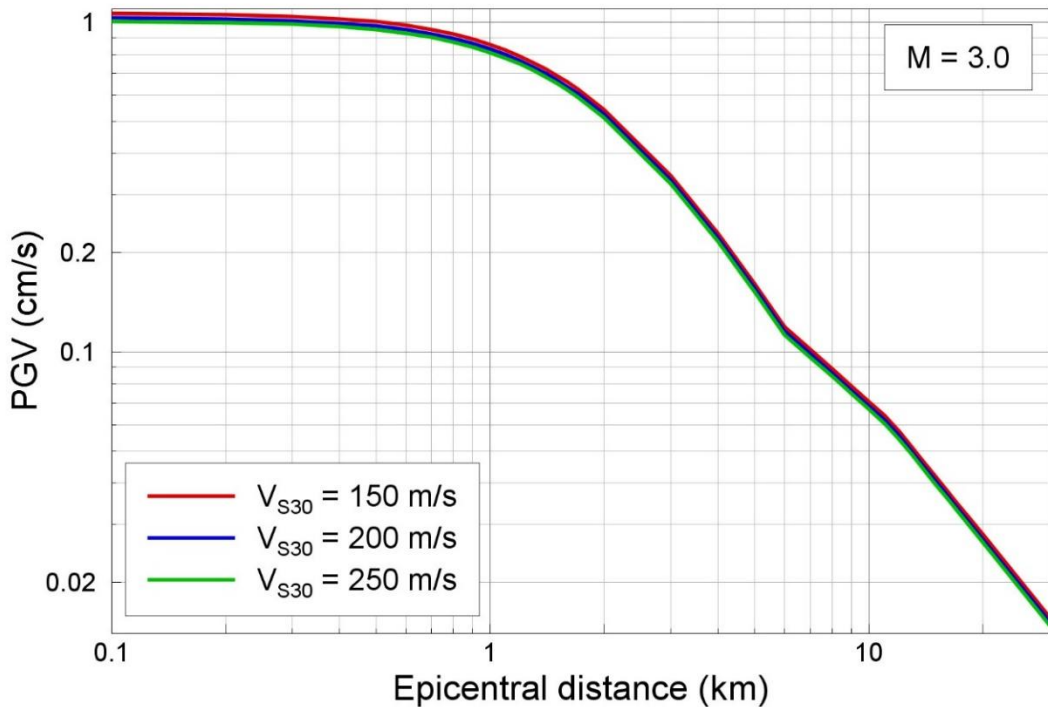


Figure 3.1. Predicted median values of geometric mean PGV from the preliminary model developed in April 2016, showing the very weak dependence on  $V_{S30}$

### 3.2. Regression analyses and results

Maximum likelihood regression was performed to find the coefficients of the functional form present in Section 3.1 for all three PGV definitions. The results are summarized in Table 3.1.

Table 3.1. Coefficients of Eqs. (3.1-3.3) for the prediction of PGV

Coefficient	$\text{PGV}_{\text{GM}}$	$\text{PGV}_{\text{Larger}}$	$\text{PGV}_{\text{MaxRot}}$
$C_1$	-5.3737	-4.8592	-4.7572
$C_2$	2.2158	2.2368	2.2472
$C_4$	-1.8422	-2.0261	-2.0650
$C_{4a}$	-1.1808	-1.1532	-1.1441
$C_{4b}$	-2.0937	-2.2237	-2.2048

Analysis of the residuals for all three equations, separated into event-terms (earthquake-to-earthquake variability) and within-event residuals, were examined with respect to magnitude and distance, respectively (Figure 3.2). No discernible trends were identified in the residuals, which suggests that the model provides an unbiased fit to the data and that the functional form, therefore, is appropriate.

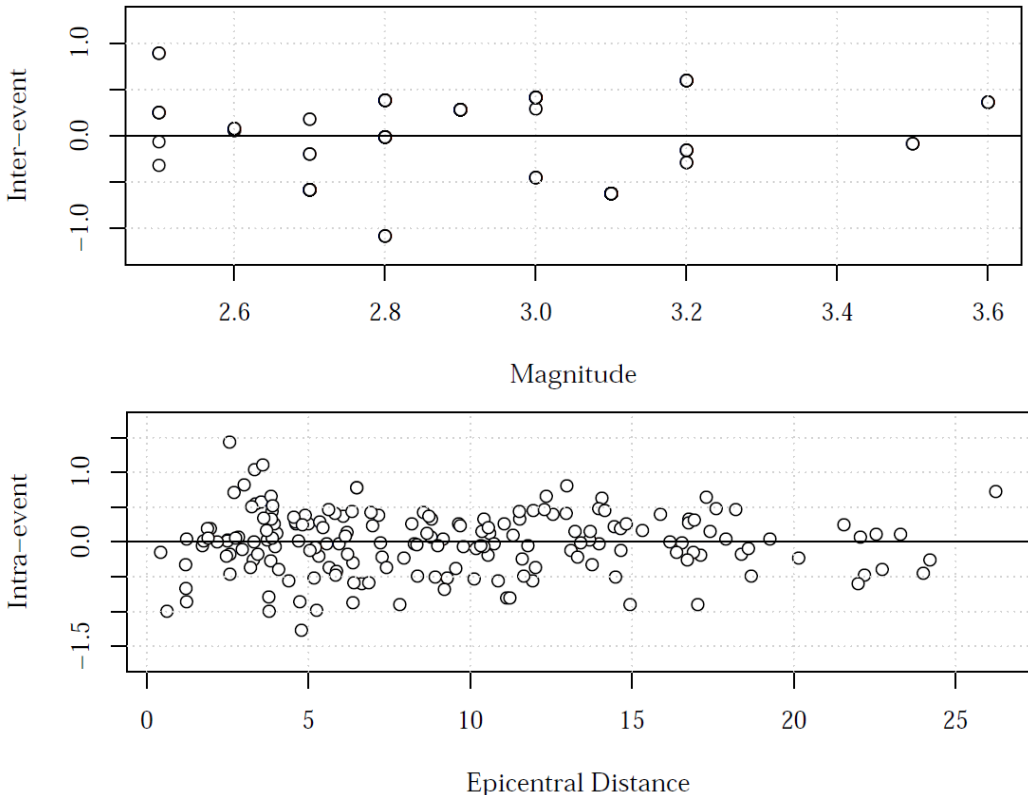


Figure 3.2. Logarithmic residuals of PGV: inter-event residuals against magnitude (*upper*) and intra-event residuals against distance (*lower*)

The standard deviations of the residuals are an integral part of the equations, which predict probabilistic distributions of PGV rather than deterministic estimates of unique values. The total standard deviation,  $\sigma$ , is decomposed into a between-earthquake component,  $\tau$ , and a within-earthquake component,  $\phi$ ; these are related as follows:

$$\sigma = \sqrt{\tau^2 + \phi^2} \quad (3.4)$$

The values of the standard deviations are reported in Table 3.2. The values are rather large but broadly comparable with small-magnitude values obtained from other empirical GMPEs. A surprising feature, noted also in the current GMM (Bommer *et al.*, 2016) is the large between-earthquake variability, which for the main GMM has been shown to result from a small number of sparsely-recorded events.

Table 3.2. Standard deviations of the PGV prediction models

Coefficient	$\text{PGV}_{\text{GM}}$	$\text{PGV}_{\text{Larger}}$	$\text{PGV}_{\text{MaxRot}}$
$\tau$	0.4837	0.4978	0.4887
$\phi$	0.4660	0.5015	0.5081
$\sigma$	0.6717	0.7066	0.7050

The fact that the smallest standard deviations are found for the geometric mean component is unsurprising, since this is a common feature among GMPEs. The reason for this feature is that this definition effectively removes the component-to-component variability, which has been found to be rather large for recorded ground motions in the Groningen field (Bommer *et al.*, 2016).

### 3.3. Predictions of PGV

Figure 3.3 shows predicted median values of PGV from the three equations as a function of epicentral distance for three magnitudes that cover the likely range of application of these equations. Most observations that can be made regarding these plots are rather obvious and correspond to features that are fully expected. Firstly, the predicted values of geometric mean PGV are appreciably lower than the values from the other two models. The largest values are obtained from the maximum rotated component model, but these are only marginally bigger than the larger component values. There is a clear scaling of the PGV values with magnitude visible in all three models (note that the y-axes are not the same on all three frames). In all three models, the magnitude scaling coefficient,  $c_2$ , is close to 2.2, which suggests an increase in PGV by a factor of about 9 due to a unit increase of earthquake magnitude. In practice, this is slightly offset at short distances due to the corresponding increase in the near-source distance saturation value from Eq.(3.2).

The distance scaling is quite rapidly, particularly at short distances, even though this is not immediately obvious from these plots of log-log axes. For magnitude 3 earthquake, the median PGV values are expected to be reduced by an order of magnitude as the waves propagate from about 2 km to 11 km epicentral distance.

Figure 3.4 shows the same information as Figure 3.3 except that in place of the median (50-percentile) values of PGV, 84-percentile predictions—obtained by adding one standard deviation—are shown. The patterns are essentially the same as those observed for the median values but the amplitudes are at least twice as high. The differences between the larger and maximum rotated values of PGV are a little smaller than for the median predictions as a result of the slightly larger total sigma associated with the latter definition.

The largest predicted median values are consistent with those in the database. At the 84-percentile level, the maximum rotated PGV at the epicentre is on the order of 7.4 cm/s. Also noteworthy is the fact the predicted values decay to very low levels well within the dimensions of the Groningen field. The median predictions of the ‘maximum’ components fall below the 0.01 cm/s level around 50 km from the epicentre of a magnitude 3.5 earthquake.

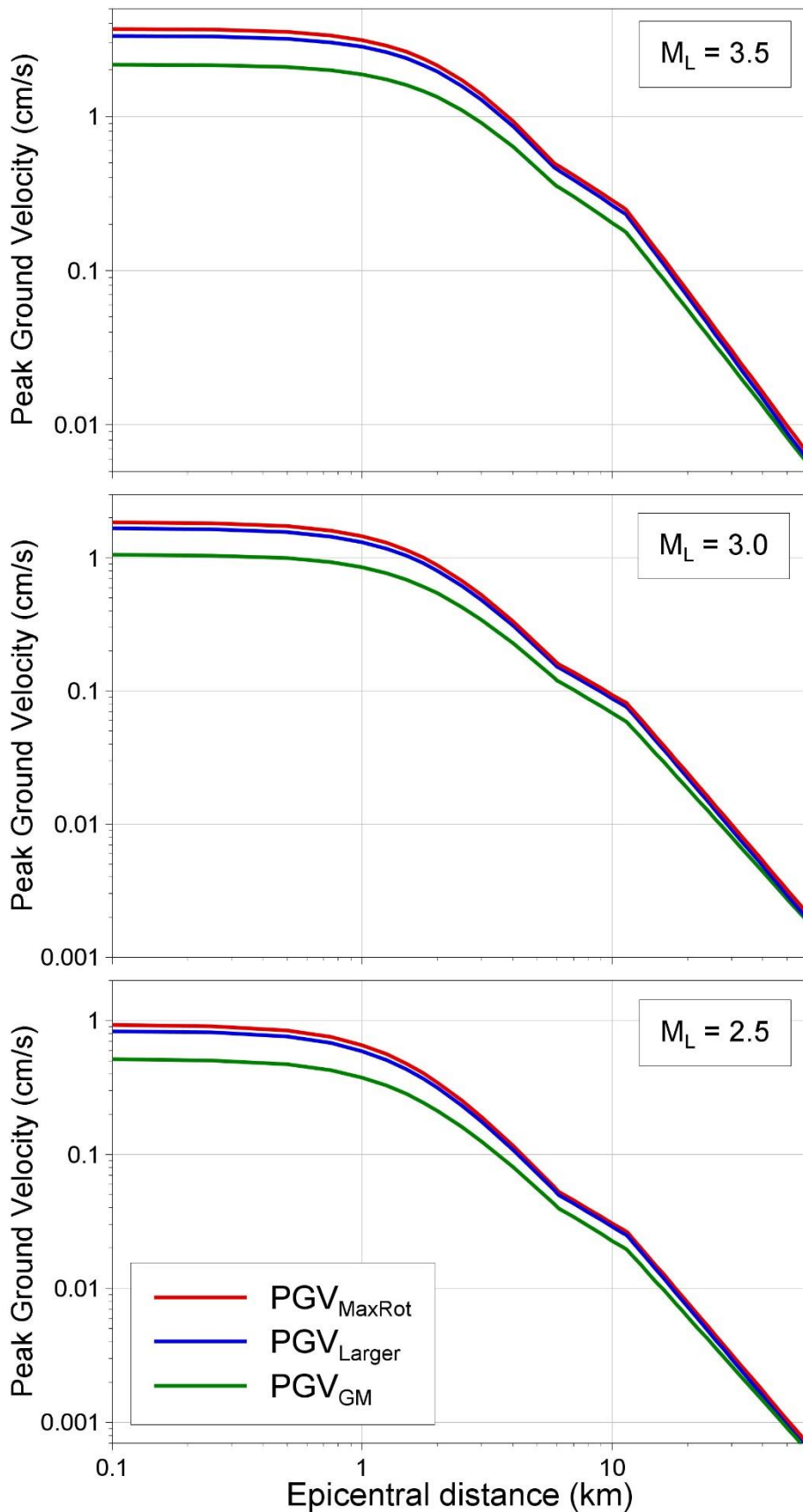


Figure 3.3. Predicted median PGV values against distance for three magnitudes

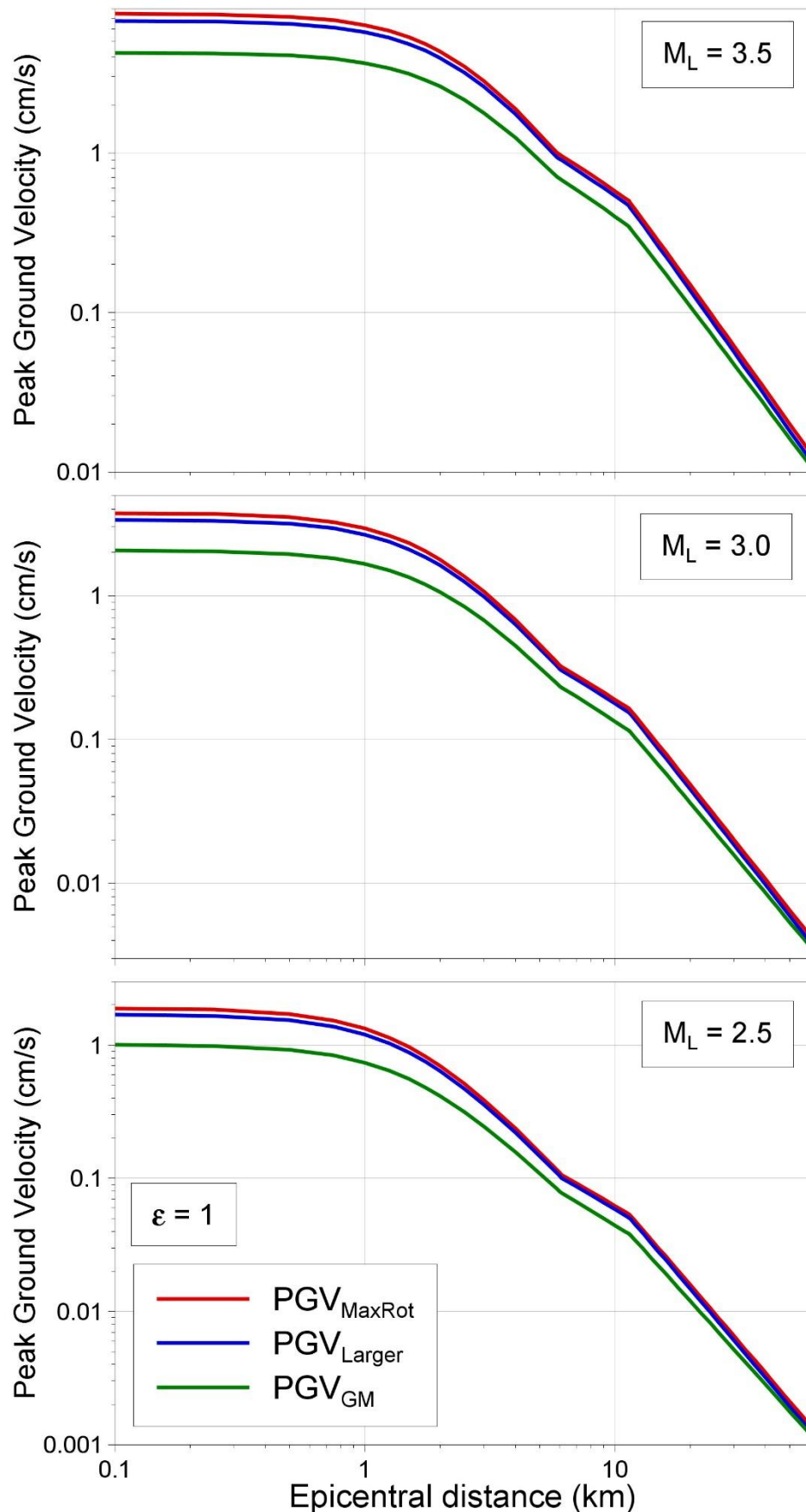


Figure 3.4. Predicted 84-percentile PGV values against distance for three magnitudes

## 4. Concluding Remarks

New empirical PGV equations calibrated to the Groningen field have been derived, using three different definitions of the horizontal component of motion: the geometric mean of the two horizontal components, the larger of the two horizontal components, and the maximum component identified by rotation of the recorded traces. The models for these three definitions predict progressively larger values of PGV.

The new PGV equation presented herein can be used with confidence to estimation peak ground velocity on the Groningen field for earthquakes with magnitudes from 2.5 to 3.6. The model could be extrapolated beyond these limits, perhaps to 2 at the lower end and 4 at the upper end, but certainly no farther, due to the purely linear magnitude scaling in the model, which would not be appropriate for a broader magnitude range (e.g., Douglas & Jousset, 2011; Baltay & Hanks, 2014). The equation can be applied with confidence up to 30 km and probably with reasonable confidence to 50 km.

The equations include coefficients for the prediction of the median values of PGV and also the standard deviations to allow values to be estimated at other exceedance values.

## 5. References

- Baker, J.W. & C.A. Cornell (2006). Which spectral acceleration are you using? *Earthquake Spectra* **22**(2), 293-312.
- Baltay, A.S. & T.C. Hanks (2014). Understanding the magnitude dependence of PGA and PGV in NGA-West 2 data. *Bulletin of the Seismological Society of America* **104**(6), 2851-2865.
- Beyer, K. & J.J. Bommer (2006). Relationships between median values and aleatory variabilities for different definitions of the horizontal component of motion. *Bulletin of the Seismological Society of America* **94**(4A), 1512-1522. *Erratum: 2007, 97*(5), 1769.
- Bommer, J.J., B. Dost, B. Edwards, P.P. Kruiver, P. Meijers, M. Ntinalexis, B. Polidoro, A. Rodríguez-Marek & P.J. Stafford (2015). *Development of Version 2 GMPEs for response spectral accelerations and significant durations from induced earthquakes in the Groningen field*. Version 2, 29 October, 515 pp.
- Bommer, J.J., B. Dost, B. Edwards, P.P. Kruiver, P. Meijers, M. Ntinalexis, A. Rodríguez-Marek & P.J. Stafford (2016). *Development of V3 GMPEs for response spectral accelerations and significant durations from induced earthquakes in the Groningen field*. Version 0, 8 July, 476 pp.
- Douglas, J. & P. Jousset (2011). Modeling the difference in ground-motion magnitude-scaling in small and large earthquakes. *Seismological Research Letters* **82**(4), 504-508.
- SBR (2002). *Schade aan gebouwen meet-en beoordingsrichtlijn, Deel A*. 38 pp.
- Watson-Lamprey, J.A. & D.M. Boore (2007). Beyond  $\text{Sa}_{\text{GMRot}}$ : Conversion to  $\text{Sa}_{\text{arb}}$ ,  $\text{Sa}_{\text{SN}}$ , and  $\text{Sa}_{\text{MaxRot}}$ . *Bulletin of the Seismological Society of America* **97**(5), 1511-1524.